Rapid One-Pot Synthesis of Pyrrole-Appended Isocorroles

Simon Larsen,[a] Laura J. M[c]Cormick[b] and Abhik Ghosh*,[a]

[a] Department of Chemistry, UiT – The Arctic University of Norway, 9037 Tromsø, Norway;
E-mail: abhik.ghosh@uit.no (AG)
[b]Advanced Light Source, Lawrence Berkeley National Laboratory,
Berkeley, CA 94720-8229, USA

Abstract. Free-base meso-triarylcorroles have been found to undergo oxidative coupling with an excess of pyrrole in dichloromethane in the presence of 2,3-dichloro-5,6-dicyano-1,4-benzoquinone (DDQ) affording 5/10-pyrrole-appended isocorroles in reasonable yields (35-60 %) and in a matter of seconds. The free-base isocorrole ligands could all be complexed to copper with $Cu(OAc)_2 \cdot H_2O$ in chloroform/methanol in 55-80 % yields. Single-crystal X-ray structures of two of the new compounds (H_2[5-pyr-T*p*OMePiC] and Cu[10-pyr-T*p*OMePiC]) revealed planar macrocycles with rms atomic displacements of only 0.02 and 0.06 Å relative to their respective best-fit $C_{19}N_4$ planes. Both free-base and Cu(II)-complexed isocorroles exhibit richly featured UV-vis-NIR spectra with red/NIR absorption maxima at ~650 nm and ~725 nm for the free-bases and ~800-850 nm for the copper complexes, suggesting potential applications in photodynamic therapy.

Note: The crystal structures described herein have CCDC deposition numbers CCDC 1847337-1847338.

Introduction. Over the last quarter-century, during which the chemistry of corroles has grown by leaps and bounds,[1,2,3] isocorroles have to some extent languished in the shadow of their better-known isomers. Nevertheless, a string of papers over the last decade have highlighted their potential importance.[4,5,6,7] They are relatively stable and practical to work with. They are also increasingly accessible, albeit in rather variable yields, via simple derivatization of corroles.[4,8,9] Moreover, by combining a porphyrin-like 2– charge with a corrole-like, sterically constrained N_4 core, isocorroles and heteroisocorroles[10,11] provide novel platforms for coordination chemistry.[12,13] Finally, as homoconjugated and potentially homoaromatic[14] compounds, they exhibit surprisingly porphyrin-like electronic absorption spectra that extend well into the near-infrared (NIR), potentially heralding applications in photodynamic therapy.[15,16] Here we report that *meso*-pyrrole–appended isocorroles may be obtained in reasonable yields via brief, room-temperature oxidative coupling of a free-base *meso*-triarylcorrole and pyrrole (Scheme 1).[17,18,19] Both 5- and 10-isocorroles were obtained, with the former predominating. Unambiguous proof of structure came from two single-crystal X-ray diffraction analyses, one for a free-base 5-isocorrole and the other for a Cu(II) 10-isocorrole.

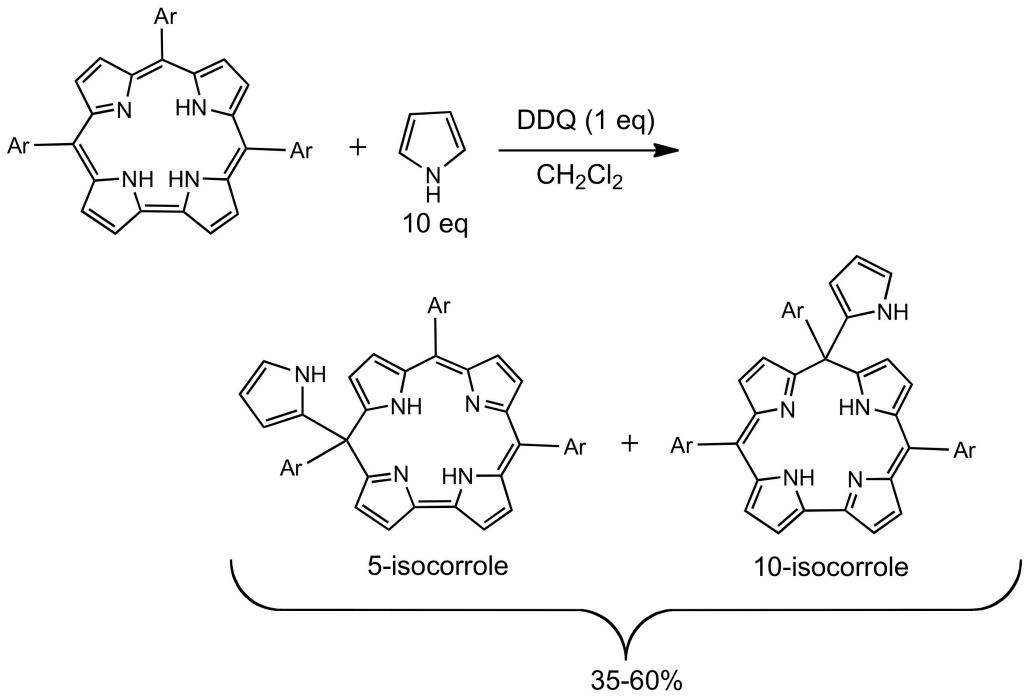

Scheme 1

Results and discussion. The free-base compounds described here were first observed as products of pyrrole-aldehyde condensations,[1,20] particularly reaction conditions with a large excess of pyrrole. Mass spectrometric analyses indicated pentapyrrolic products with a molecular formula equivalent to 'pyrrole + corrole – 2H', apparently consistent with an isosmaragdyrin. One of these products fortunately proved amenable to single-crystal X-ray structure determination, clearly indicating a 5-(2-pyrrolyl)isocorole (as opposed to an isosmaragdyrin). With the nature of the products established, we devised an alternative, more convenient route based on the oxidative coupling of a corrole and pyrrole. According to the final protocol, a *meso*-tris(*para*-X-phenyl)corrole, H_3[T*p*XPC], where X ⊂ {CF_3, H, Me, OMe}, and pyrrole underwent immediate coupling in dichloromethane in the presence of 2,3-dichloro-5,6-dicyano-1,4-benzoquinone (DDQ). Both the 5- and 10-(2-pyrrolyl)isocorrole isomers were obtained, denoted hereafter as H_2[5/10-pyr-T*p*XPiC], with the 5-isomer accounting for ≳ 90% of the combined yield, which ranged from about 35-40% for X = CF_3 and H to about 60% for X = Me and OMe. The free ligands were also complexed to Cu(II) using $Cu(OAc)_2 \cdot H_2O$ (Ac = acetyl) in 4:1 v/v mixture of chloroform/methanol as solvent. The 5- and 10- regioisomers of both the free bases and Cu(II) complexes could be separated via preparative thin layer chromatography.

The ^{1}H NMR spectra of the eight free-base isocorroles could each be fully assigned, as depicted in Figure 1 for H_2[5-pyr-T*p*OMePiC]. The chemical shifts of all the *β*- and *meso*-aryl protons, including the *meso*-pyrrolyl CH protons, were found to range from about 5.9 to 7.5 ppm, while the *meso*-pyrrolyl NH proton was found at ~8.1 ppm. Using the latter peak as a starting point, COSY analysis led to the assignment of the other *meso*-pyrrolyl protons. NOESY analysis then identified the nearby *meso*-aryl and *β* protons, with the remainder of the peaks identified via a combination of COSY and NOESY analysis. The two inner NH protons were located at 14.83 ± 0.3 ppm, suggesting a net global paratropic current. Such a proposition is in line with recent DFT calculations of magnetically induced current densities indicating that, while unsubstituted isocorrole is homoaromatic,[15,16] substituents at the saturated *meso* carbon can dramatically affect the global ring current. Substituted isocorroles accordingly may range from homoaromatic to antihomoaromatic.

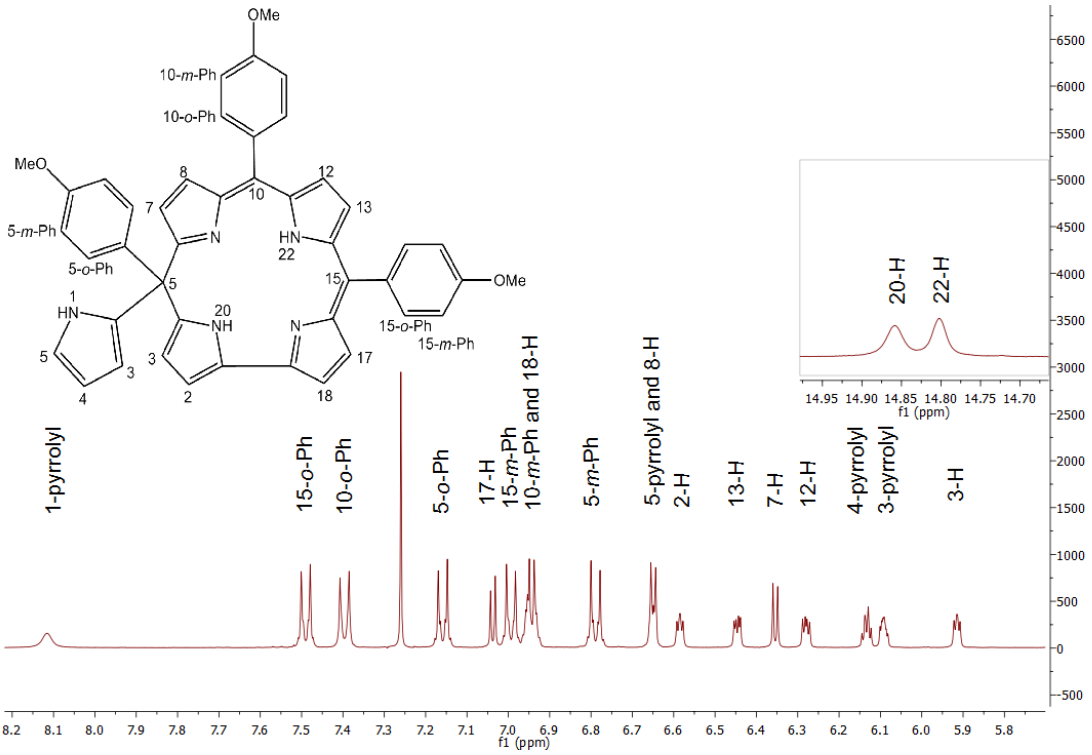

Figure 1. The ^{1}H NMR spectrum of H_2[5-pyr-T*p*OMePiC].

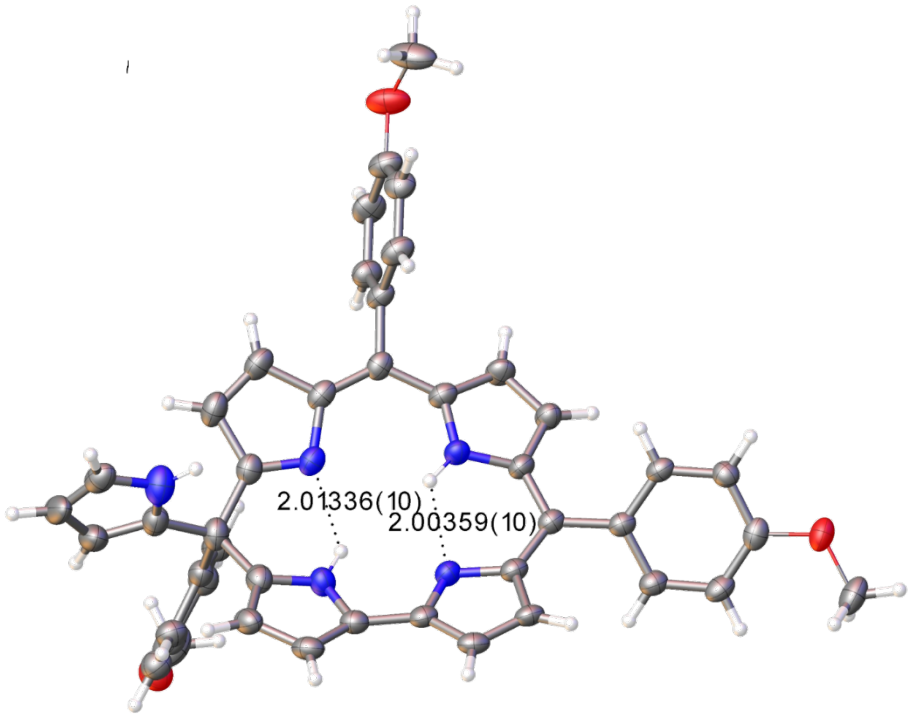

Figure 2. Thermal ellipsoid plot for H_2[5-pyr-T*p*OMePiC], including key hydrogen bond distances.

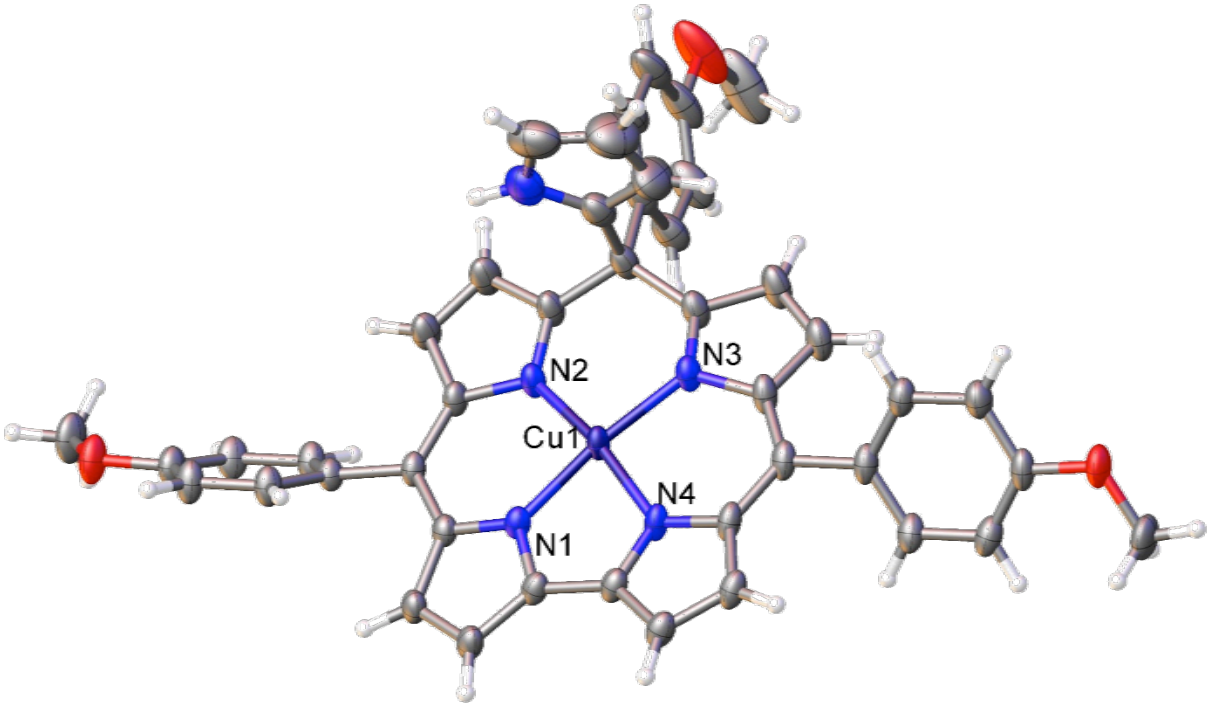

Figure 3. Thermal ellipsoid plot for Cu[10-pyr-T*p*OMePiC]. Selected distances (Å): Cu1-N1 1.915(3), Cu1-N2 1.925(3), Cu1-N3 1.925(3), and Cu1-N4 1.921(3).

Single-crystal X-ray structures could be obtained for two of the compounds prepared, H_2[5-pyr-T*p*OMePiC] (Figure 2) and Cu[10-pyr-T*p*OMePiC] (Figure 3). Like other isocorrole structures reported to date,[4-9] both compounds exhibit remarkably planar macrocycles with rms atomic displacements of only 0.02 and 0.06 Å relative to their respective best-fit $C_{19}N_4$ planes. The relative planarity of the Cu complex may be contrasted with the saddled geometries of Cu corroles, in which the saddling is thought to reflect a noninnocent Cu^{II}-corrole$^{\bullet 2-}$ description.[21,22,23,24,25,26,27,28,29] Not surprisingly, the observed Cu-N distances (1.915-1.925 Å) are intermediate between those observed for typical Cu triarylcorroles and Cu porphyrins.[2,30] Aside from these, the other bond distances do not warrant much comment, the skeletal C-C and C-N bond distances being typical of those observed for dipyrrins.

Table 1. Crystallographic data for H_2[5-pyr-T*p*OMePiC] and Cu[10-pyr-T*p*OMePiC].

Sample	H_2[5-pyr-T*p*OMePiC]•dichloromethane	Cu[10-pyr-T*p*OMePiC]•chloroform
Chemical formula	$C_{45}H_{37}Cl_2N_5O_3$	$C_{45}H_{34}Cl_3CuN_5O_3$
Formula mass	766.69	862.66
Crystal system	triclinic	triclinic
Crystal size (mm^3)	0.230 x 0.030 x 0.010	0.150 x 0.080 x 0.070
Space group	P -1	P -1
λ (Å)	0.7749	0.7749
a (Å)	9.7321(6	11.1767(16)
b (Å)	12.1142(7)	11.6310(16)
c (Å)	16.7703(10)	15.297(2)
a (deg)	85.618(2)	104.788(3)
β (deg)	85.655(2)	91.215(3)
g (deg)	70.199(2)	96.469(3)
Z	2	2
V ($Å^3$)	1852.20(19)	1907.9(5)
Temperature (K)	100(2)	100(2)
Density (g/cm^3)	1.375	1.502
Measured reflections	24592	94061
Unique reflections	4811	10084
Parameters	554	570
Restraints	46	56
R_{int}	0.0583	0.0568
θ range (deg.)	1.330 to 24.614	1.503 to 31.849
R_1, wR_2 all data	0.0970, 0.2092	0.0842, 0.2105
S (GooF) all data	1.133	1.026
Max/min res. dens. ($e/Å^3$)	0.474 /-0.538	1.383/-1.674

Both the free-base and Cu(II)-complexed isocorroles exhibit richly featured UV-vis-NIR spectra (Figure 4-7). All the compounds exhibit a strong "Soret" band in the 400-500 nm region as well as one or more sharp post-Soret features in the near-UV. More notably, compared with their free-base precursors, the Cu isocorrole derivatives exhibit significantly more redshifted Soret maxima, by a margin of a few tens of nm. The compounds also exhibit strong "Q" bands. For the free base isocorroles, these are broad, double-humped features plateauing within approximately 650-725 nm. The Q bands of the Cu complexes are also double humped, but sharper and redshifted into the near-IR, with the most intense peaks occuring at ~855 nm for the 5-regioisomers and ~800 nm for the 10-regioisomers. We tentatively suggest that the considerably redshifted spectra of the Cu complexes relative to the free bases might reflect ligand-to-metal charge transfer transitions. That said, the optical properties of isocorrole derivatives clearly deserve more in-depth study, both via the synthesis of new complexes and via quantum chemical means.[15] The potential for new isocorrole-based sensitizers for photodynamic therapy is indeed considerable.

Table 2. UV-vis absorption maxima (nm) and molar absorptivities (ϵ x 10^{-4}, $M^{-1}cm^{-1}$) in dichloromethane solution.

	< 450 nm	450-600 nm	>600 nm
H_2[5-pyr-T*p*OCH_3PiC]	345 (2.05), 415 (6.00)	–	660 (0.76), 708 (0.72).
H_2[5-pyr-T*p*MePiC]	345 (2.97), 406 (5.61)	–	661 (0.82), 705 (0.79)
H_2[5-pyr-TPiC]	339 (2.94), 407 (4.72)	–	661 (0.71), 705 (0.69
H_2[5-pyr-T*p*CF_3PiC]	338 (2.71), 407 (4.06)	–	661 (0.73), 706 (0.74)
H_2[10-pyr-T*p*OCH_3PiC]	375 (2.61), 434 (4.71)	–	656 (0.69), 698 (0.69)
H_2[10-pyr-T*p*MePiC]	359 (1.86), 432 (3.16)	–	658 (0.44), 699 (0.45)
H_2[10-pyr-TPiC]	351 (1.41), 430 (2.58)	–	656 (0.37), 691 (0.36)
H_2[10-pyr-T*p*CF_3PiC]	347 (0.89), 429 (1.94)	–	648 (0.29), 700 (0.26)
Cu[5-pyr-T*p*OCH_3PiC]	368 (2.42)	459 (3.80), 556 (0.69)	786 (0.59), 862 (0.77)
Cu[5-pyr-T*p*MePiC]	285 (1.60), 361 (3.00)	459 (3.61), 557 (0.65)	793 (0.65), 860 (0.85)
Cu[5-pyr-TPiC]	296 (1.41), 357 (2.68)	459 (3.13), 557 (0.57)	792 (0.58), 856 (0.80)
Cu[5-pyr-T*p*CF_3PiC]	308 (1.83), 357 (2.67)	465 (3.44), 560 (0.63)	792 (0.67), 858 (0.98)
Cu[10-pyr-T*p*OCH_3PiC]	271 (1.38), 387 (2.76)	470 (3.50), 544 (0.34)	726 (0.34), 800 (0.78)
Cu[10-pyr-T*p*MePiC]	315 (1.23), 370 (2.81)	468 (3.49), 539 (0.38)	728 (0.33), 800 (0.80)
Cu[10-pyr-TPiC]	305 (0.87), 361 (1.28)	470 (1.96), 540 (0.21)	729 (0.18), 800 (0.44)
Cu[10-pyr-T*p*CF_3PiC]	302 (1.42), 356 (1.39), 388 (1.31)	474 (2.62), 545 (0.24)	734 (0.27), 806 (0.62)

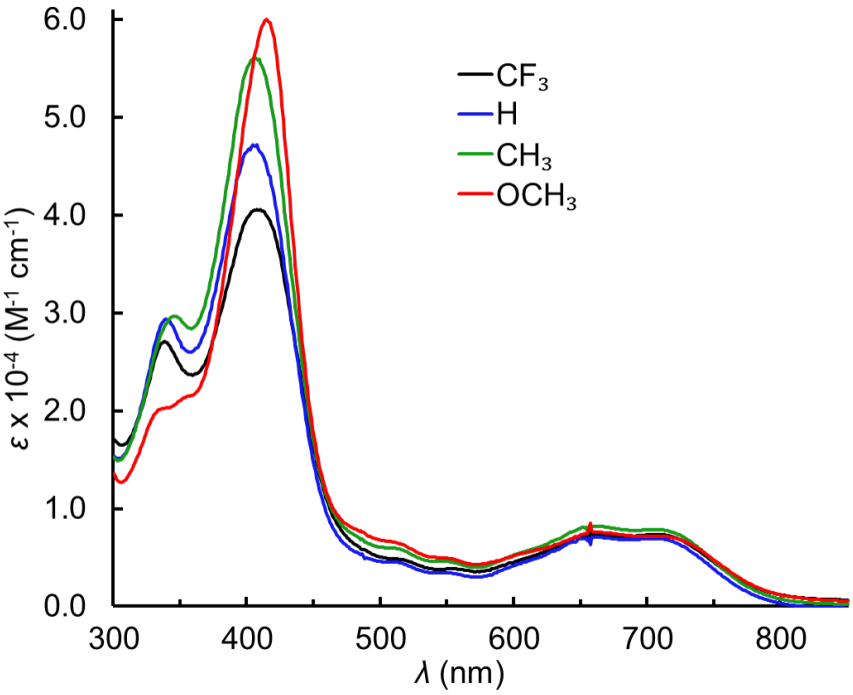

Figure 4. UV-visible spectra of H_2[5-pyr-T*p*XPiC], where X $\subset$ {CF_3, H, Me, OMe}.

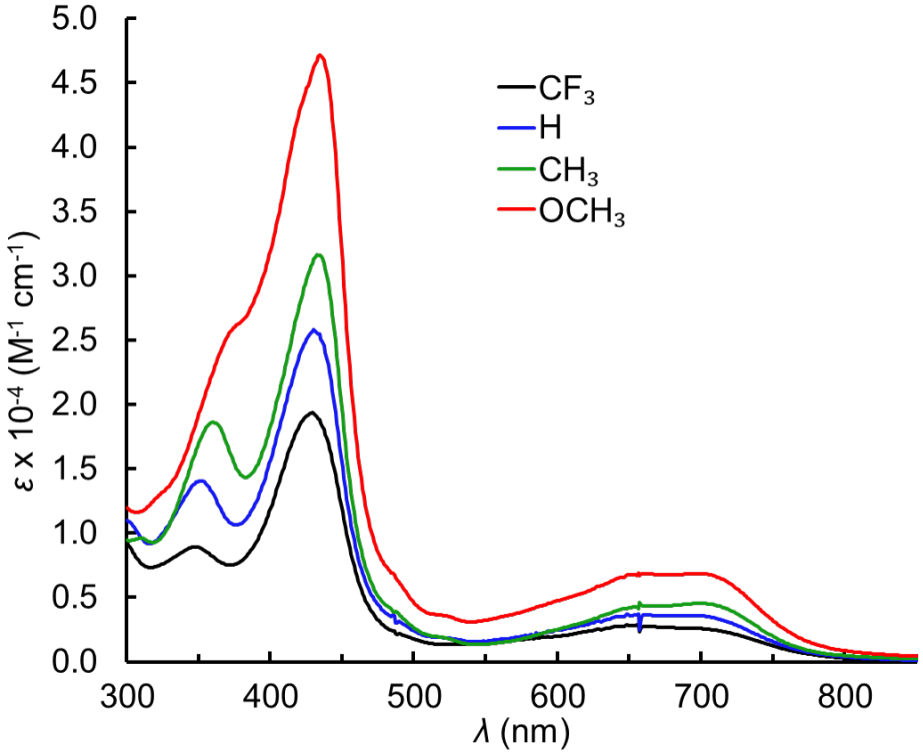

Figure 5. UV-visible spectra of H_2[10-pyr-T*p*XPiC], where X ⊂ {CF_3, H, Me, OMe}.

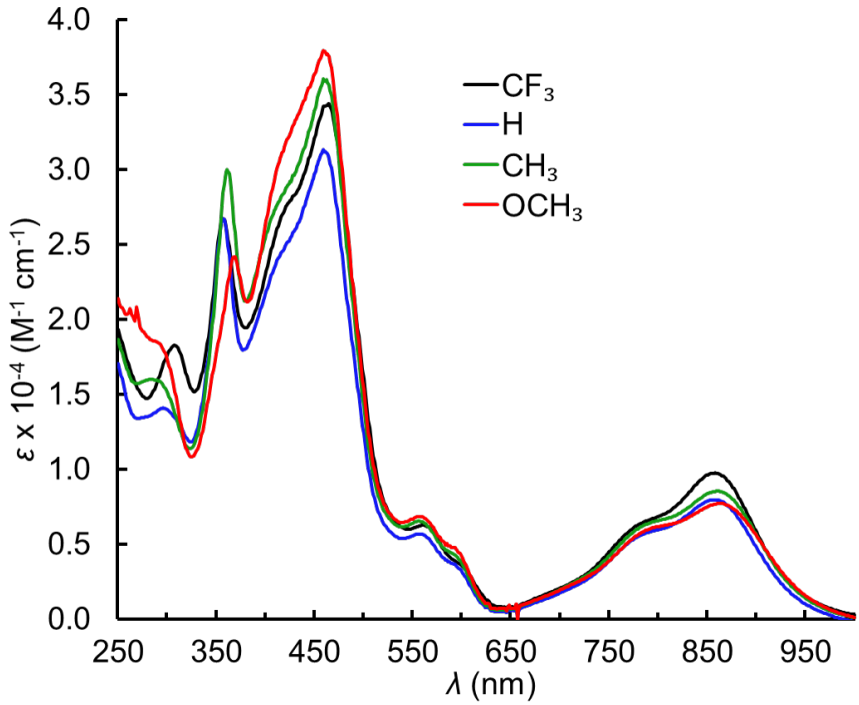

Figure 6. UV-visible spectra of Cu[5-pyr-T*p*XPiC], where X ⊂ {CF_3, H, Me, OMe}.

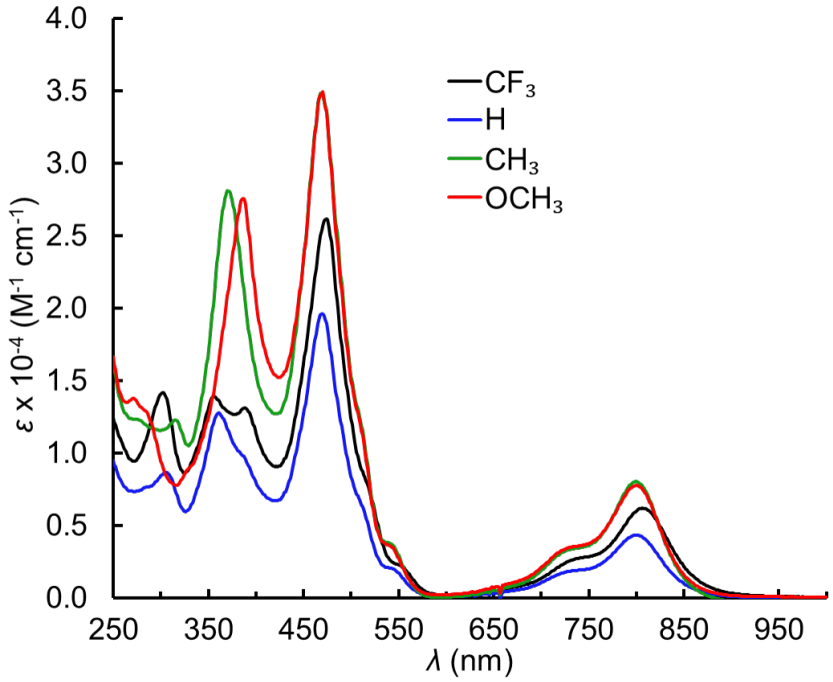

Figure 7. UV-visible spectra of Cu[10-pyr-T*p*XPiC], where X ⊂ {CF_3, H, Me, OMe}.

Cyclic voltammetry on the four Cu(II) 5-isocorroles and on Cu[10-pyr-T*p*CF_3PiC] revealed fully reversible redox cycles with multiple oxidation and reduction features (Figure 8 and Table 3). Interestingly, the 5-isocorrole series was found to exhibit an isolated oxidation peak 0.74 ± 0.05 V vs. SCE with no nearby, corresponding reduction peak and a reduction peak at -0.21 ± 0.9 V vs. SCE with no nearby, corresponding oxidation peak. It is reasonable to suppose that oxidation leads to a persistent π-cation radical, potentially involving the pendant pyrrole, which is reduced at a much more negative potential relative to the oxidation peak potential. In contrast, the 10-isocorrole complex Cu[10-pyr-T*p*CF_3PiC] was found to exhibit normal, reversible oxidation and reduction features. Interestingly, the second reduction peak of the 5-isocorrole series (labeled $E_{red,b}$ in Table 2) occurs at the same potential as the first reduction of *meso*-methoxy isocorrole complexes Cu[5/10-MeO-T*p*CH_3PiC] studied by Pomarico *et al.* and therefore by analogy may be tentatively assigned to a reduction leading to the molecular anion.[4] Detailed spectroelectrochemical and density functional theory-based computational studies are currently in progress, which should result in full assignment of the electrochemical features observed here.[4]

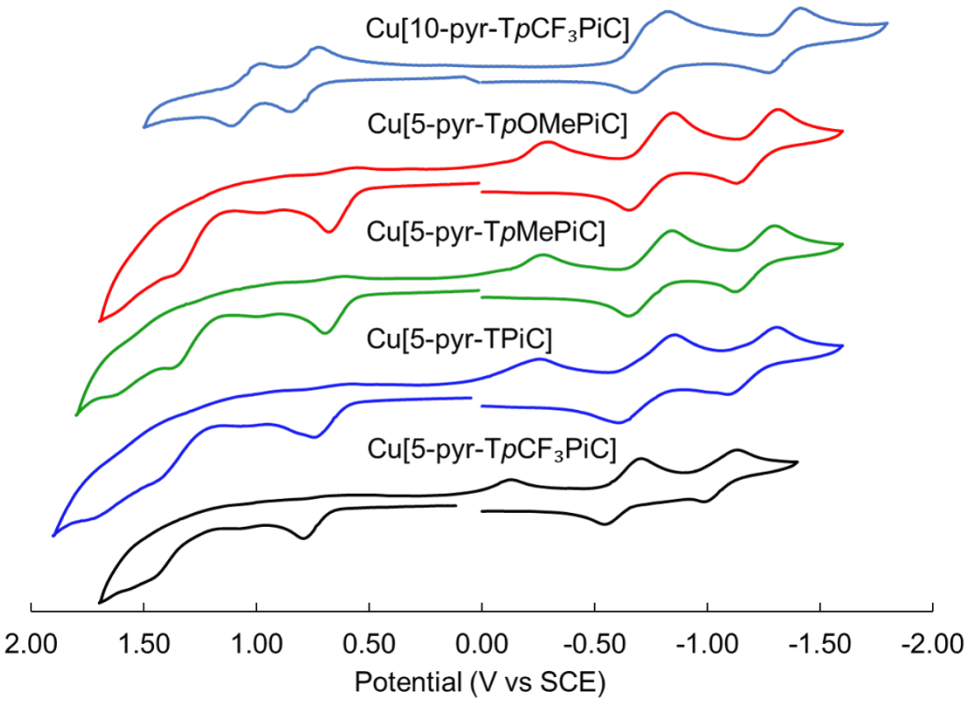

Figure 8. Cyclic voltammograms of selected Cu isocorrole complexes in CH_2Cl_2 containing 0.1 M TBAP. Scan rate = 100 mV/s.

Table 3. Redox potentials (V vs. SCE) of selected Cu isocorrole derivatives. in CH_2Cl_2 containing 0.1 M TBAP. Scan rate = 100 mV/s.

Compound	$E_{ox,b}$	$E_{ox,a}$	$E_{red,a}$	$E_{red,b}$	$E_{red,c}$	ΔE
Cu[10-pyr-T*p*CF_3PiC]	1.05	0.79	–	-0.75	-1.34	1.54
Cu[5-pyr-T*p*OCH_3PiC]	–	0.68[a]	-0.29[a]	-0.75	-1.23	0.97
Cu[5-pyr-T*p*CH_3PiC]	–	0.70[a]	-0.27[a]	-0.75	-1.22	0.97
Cu[5-pyr-TPiC]	–	0.74[a]	-0.26[a]	-0.74	-1.20	1.00
Cu[5-pyr-T*p*CF_3PiC]	–	0.79[a]	-0.13[a]	-0.63	-1.06	0.92

[a] Peak potential

Conclusion. Interaction of free-base *meso*-triarylcorroles with an excess of pyrrole in the presence of DDQ in dichloromethane at room temperature results in moderate yields (35-60%) of 5/10-(2-pyrrolyl)isocorroles in a matter of seconds. Metal coordination to each isocorrole ligand was demonstrated by complexation with Cu(II). Both the free ligands and their metal complexes were found to exhibit strong absorption in the near-infrared, promising potential applications as sensitizers in photodynamic therapy.

Experimental section

Materials. All free-base corroles were synthesized via the now-standard water-methanol method.[31] All reagents, except pyrrole, were purchased from Sigma-Aldrich and used as received. Pyrrole was passed through basic alumina (aluminium oxide 60, active basic activity I, 0.063-0.200 mm particle size, 70-230 mesh, Merck) and stored in the freezer. Silica gel 60 (0.04-0.063 mm particle size, 230-400 mesh, Merck) was employed for flash chromatography. Silica gel 60 preparative thin-layer chromatographic plates (20 cm x 20 cm x 0.5 mm, Merck) were used for final purification of all compounds.

General instrumental methods. UV-visible spectra were recorded on an HP 8453 spectrophotometer. ^{1}H NMR spectra were recorded on a 400 MHz Bruker Avance III HD spectrometer equipped with a 5 mm BB/1H SmartProbe and referenced to either residual CH_2Cl_2 at 5.32 ppm or residual $CHCl_3$ at 7.26 ppm. High-resolution electrospray-ionization (HR-ESI) mass spectra were recorded on an LTQ Orbitrap XL spectrometer, using methanolic solutions and typically in positive ion mode. Elemental analyses were performed by Atlantic Microlab Inc., U.S.A.[32]

Cyclic voltammetry was carried out at 298 K with an EG&G Model 263A potentiostat equipped with a three-electrode system: a glassy carbon working electrode, a platinum wire counterelectrode, and a saturated calomel reference electrode (SCE). Tetra(*n*-butyl)ammonium perchlorate (*CAUTION!*), recrystallized twice from absolute ethanol and dried in a desiccator for at least 2 weeks, was used as the supporting electrolyte. Anhydrous CH_2Cl_2 (Aldrich) was used as solvent. The reference electrode was separated from the bulk solution by a fritted-glass bridge filled with the solvent/supporting electrolyte mixture. The electrolyte solution was purged with argon for at least 2 min prior to all measurements, which were carried out under an argon blanket. All potentials were referenced to the SCE.

General procedure for preparation of free-base 5/10-(2-pyrrolyl)isocorroles . A 100-mL round-bottom flask equipped with a magnetic stirring bar was charged with a free-base *meso*-triarylcorrole (20-25 mg) and dichloromethane (10 ml). To the stirred, degassed solution under argon were added DDQ (1 eq) and pyrrole (10 eq) in succession, whereupon the color of the solution turned olive-green within seconds. The reaction mixture was then passed through a silica plug with dichloromethane to yield the crude product as a mixture of the 5- and 10-isomer. Separation of the two regioisomers was accomplished with preparative thin-layer

chromatography employing the following solvents: dichloromethane/*n*-hexane (8:1) for X = *p*-OCH_3, dichloromethane/*n*-hexane (2:1) for *p*-CH_3, dichloromethane/pentane (1:1) for *p*-H, and dichloromethane/pentane (1:2) for *p*-CF_3. In the event the isomers did not separate, the isocorrole band was divided in fractions and prep-TLC repeated on each individual fraction. The process continued until full separation was achieved. Yields and analytical details for each compound are as follows. Due to low yield of the 10-isomers, elemental analysis was only done for the 5-isomers.

5-(2-Pyrrolyl)-5,10,15-tris(4-methoxyphenyl)isocorrole: Yield 14.8 mg (56 %). UV-Vis (CH_2Cl_2) λ_{max} (nm) [ϵ x 10^{-4} ($M^{-1}cm^{-1}$)]: 345 (2.05), 415 (6.00), 660 (0.76), 708 (0.72). ^{1}H NMR (400 MHz, $CDCl_3$, δ): 14.86 (s, 1H, NH), 14.80 (s, 1H, NH), 8.12 (s, 1H, 1-pyrrolyl), 7.49 (d, *J* = 8.8 Hz, 2H, 15-*o*-Ph), 7.40 (d, *J* = 8.8 Hz, 2H, 10-*o*-Ph), 7.16 (d, *J* = 8.9 Hz, 2H, 5-*o*-Ph), 7.04 (d, *J* = 4.5 Hz, 1H, *β*-H), 6.99 (d, *J* = 8.8 Hz, 2H, 15-*m*-Ph), 6.96 – 6.91 (m, 3H, overlapping 10-*m*-Ph and *β*-H), 6.79 (d, *J* = 8.8 Hz, 2H, 5-*m*-Ph), 6.67 – 6.63 (m, 2H, overlapping *β*-H and 5-pyrrolyl), 6.58 (dd, *J* = 3.6, 2.5 Hz, 1H, *β*-H), 6.45 (dd, *J* = 4.2, 2.0 Hz, 1H, *β*-H), 6.35 (d, *J* = 4.5 Hz, 1H, *β*-H), 6.28 (dd, *J* = 4.3, 2.5 Hz, 1H, *β*-H), 6.15 – 6.12 (m, 1H, 4-pyrrolyl), 6.10 – 6.07 (m, 1H, 3-pyrrolyl), 5.91 (dd, *J* = 3.6, 2.4 Hz, 1H, *β*-H), 3.89 (s, 3H, 15-*p*-OCH_3), 3.88 (s, 3H, 10-*p*-OCH_3), 3.78 (s, 3H, 5-*p*-OCH_3). MS (ESI) m/z: 682.2815; calcd for $C_{44}H_{35}N_5O_3H$: 682.2813 [M + H^+]. Elemental analysis: 77.45, H 5.25, N 10.09; calcd for $C_{44}H_{35}N_5O_3$: C 77.51, H 5.17, N 10.27.

10-(2-Pyrrolyl)-5,10,15-tris(4-methoxyphenyl)isocorrole: Yield 1.2 mg (4.5 %). UV-Vis (CH_2Cl_2) λ_{max} (nm) [ϵ x 10^{-4} ($M^{-1}cm^{-1}$)]: 375 (2.61), 434 (4.71), 656 (0.69), 698 (0.69). ^{1}H NMR (400 MHz, $CDCl_3$, δ): 14.72 (s, 2H, NH), 7.93 (s, 1H, 1-pyrrolyl), 7.56 (d, *J* = 8.7 Hz, 4H, 5,15-*o*-Ph), 7.04 – 6.97 (m, 6H, overlapping 5,15-*m*-Ph and 10-*o*-Ph), 6.82 (d, *J* = 8.9 Hz, 2H, 10-*m*-Ph), 6.77 (d, *J* = 4.1 Hz, 2H, *β*-H), 6.73 (d, *J* = 4.1 Hz, 2H, *β*-H), 6.68 – 6.65 (m, 1H, 5-pyrrolyl), 6.64 (d, *J* = 4.2 Hz, 2H, *β*-H), 6.11 – 6.07 (m, 1H, 4-pyrrolyl), 5.99 (d, *J* = 4.2 Hz, 2H, *β*-H), 5.85 – 5.81 (m, 1H, 3-pyrrolyl), 3.90 (s, 6H, 5,15-*p*-OCH_3), 3.80 (s, 3H, 10-*p*-OCH_3). MS (ESI) m/z: 682.2814; calcd for $C_{44}H_{35}N_5O_3H$: 682.2813 [M + H^+].

5-(2-Pyrrolyl)-5,10,15-tris(4-methylphenyl)isocorrole: Yield 17.1 mg (58 %). UV-Vis (CH_2Cl_2) λ_{max} (nm) [ϵ x 10^{-4} ($M^{-1}cm^{-1}$)]: 345 (2.97), 406 (5.61), 661 (0.82), 705 (0.79); ^{1}H NMR (400 MHz, $CDCl_3$, δ): 14.85 (s, 1H, NH), 14.79 (s, 1H, NH), 8.12 (s, 1H, 1-pyrrolyl), 7.44 (d, *J* = 8.0 Hz, 2H, 10-*o*-Ph), 7.35 (d, *J* = 7.9 Hz, 2H, 10-*o*-Ph), 7.28 (d, *J* = 7.0 Hz, 2H, 15-*m*-Ph), 7.22

(d, J = 7.2 Hz, 2H, 10-*m*-Ph), 7.14 (d, J = 8.2 Hz, 2H, 5-*o*-Ph), 7.09 – 7.02 (m, 3H, overlapping 5-*m*-Ph and *β*-H), 6.94 (d, J = 4.5 Hz, 1H, *β*-H), 6.67 – 6.62 (m, 2H, overlapping 5-pyrrole and *β*-H), 6.60 (dd, J = 2.6 Hz, 1H, *β*-H), 6.43 (dd, J = 4.3, 1.5 Hz, 1H, *β*-H), 6.37 (d, J = 4.6 Hz, 1H, *β*-H), 6.25 (dd, J = 4.5, 2.0 Hz, 1H, *β*-H), 6.15 – 6.09 (m, 2H, overlapping 3-pyrrolyl and 4-pyrrolyl), 5.92 (dd, J = 3.8, 1.7 Hz, 1H, *β*-H), 2.45 (s, 3H, 15-*p*-CH_3), 2.44 (s, 3H, 10-*p*-CH_3), 2.32 (s, 3H, 5-*p*-CH_3). MS (ESI) m/z: 634.2958; calcd for $C_{44}H_{35}N_5H$: 634.2965 [M + H^+]. Elemental analysis: C 82.68, H 5.79, N 10.59; calcd for $C_{44}H_{35}N_5$: C 83.38, H 5.57, N 11.05.

10-(2-Pyrrolyl)-5,10,15-tris(4-methylphenyl)isocorrole: Yield 0.8 mg (2.7 %). UV-Vis (CH_2Cl_2) λ_{max} (nm) [ϵ x 10^{-4} ($M^{-1}cm^{-1}$)]: 359 (1.86), 432 (3.16), 658 (0.44), 699 (0.45); ^{1}H NMR (400 MHz, $CDCl_3$ δ): 14.73 (s, 2H, NH), 7.94 (s, 1H, 1-pyrrolyl), 7.49 (d, J = 7.8 Hz, 4H, 5,15-*o*-Ph), 7.28 (d, 4H, 5,15-*m*-Ph), 7.09 (d, J = 8.1 Hz, 2H, 10-*m*-Ph), 6.99 (d, J = 7.9 Hz, 2H, 10-*o*-Ph), 6.76 (d, J = 4.1 Hz, 2H, *β*-H), 6.72 (d, J = 4.1 Hz, 2H, *β*-H), 6.67 – 6.64 (m, 1H, 2-pyrrolyl), 6.62 (d, J = 4.2 Hz, 2H, *β*-H), 6.11 – 6.08 (m, 1H, 3-pyrrolyl), 5.98 (d, J = 4.3 Hz, 2H, *β*-H), 5.87 – 5.83 (m, 1H, 4-pyrrolyl), 2.46 (s, 6H, 5,15-*p*-CH_3), 2.33 (s, 3H, 10-*p*-CH_3). MS (ESI) m/z: 634.2968; calcd for $C_{44}H_{35}N_5H$: 634.2965 [M + H^+].

5-(2-Pyrrolyl)-5,10,15-triphenylisocorrole: Yield 11.6 mg (38 %). UV-Vis (CH_2Cl_2) λ_{max} (nm) [ϵ x 10^{-4} ($M^{-1}cm^{-1}$)]: 339 (2.94), 407 (4.72), 661 (0.71), 705 (0.69). ^{1}H NMR (400 MHz, CD_2Cl_2 δ): 14.85 (s, 1H, NH), 14.81 (s, 1H, NH), 8.21 (s, 1H, 1-pyrrolyl), 7.59 – 7.55 (m, 2H, Ph), 7.52 – 7.43 (m, 8H, overlapping 5-*o*-Ph, 10-*o*-Ph and Ph), 7.33 – 7.23 (m, 5H, overlapping 15-*o*-Ph and Ph), 7.05 (d, J = 4.5 Hz, 1H, *β*-H), 7.00 (d, J = 4.5 Hz, 1H, *β*-H), 6.70 – 6.62 (m, 3H, overlapping 5-pyrrolyl and *β*-H), 6.46 (dd, J = 4.3, 1.8 Hz, 1H, *β*-H), 6.38 (d, J = 4.5 Hz, 1H, *β*-H), 6.27 (dd, J = 4.3, 2.3 Hz, 1H, *β*-H), 6.14 – 6.11 (m, 1H, 4-pyrrolyl), 6.11 – 6.08 (m, 1H, 3-pyrrolyl), 5.94 (dd, J = 2.9 Hz, 1H, *β*-H). MS (ESI) m/z: 592.2495; calcd for $C_{41}H_{29}N_5H$: 592.2496 [M + H^+]. Elemental analysis (%): C 82.60, H 5.41, N 11.15; calcd for $C_{41}H_{29}N_5$: C 83.22, H 4.94, N 11.84.

10-(2-Pyrrolyl)-5,10,15-triphenylisocorrole: Yield 1.2 mg (3.9 %). UV-Vis (CH_2Cl_2) λ_{max} (nm) [ϵ x 10^{-4} ($M^{-1}cm^{-1}$)]: 351 (1.41), 430 (2.58), 656 (0.37), 691 (0.36). ^{1}H NMR (400 MHz, $CDCl_3$ δ): 14.73 (s, 2H, NH), 7.94 (s, 1H, 1-pyrrolyl), 7.63 – 7.58 (m, 4H, 5,15-*o*-Ph), 7.50 – 7.44 (m, 6H, overlapping 5,15-*m*-Ph and 5,15-*p*-Ph), 7.34 – 7.28 (m, 3H, overlapping 10-*m*-Ph and 10-*p*-Ph), 7.13 – 7.08 (m, 2H, 10-*o*-Ph), 6.77 – 6.73 (m, 4H, overlapping *β*-H), 6.69 – 6.65

(m, 1H, 2-pyrrolyl), 6.61 (d, J = 4.3 Hz, 2H, β-H), 6.10 (q, J = 3.0 Hz, 1H, 3-pyrrolyl), 5.97 (d, J = 4.3 Hz, 2H, β-H), 5.87 – 5.84 (m, 1H, 4-pyrrolyl). MS (ESI) m/z: 592.2499; calcd for $C_{41}H_{29}N_5H$: 592.2496 [M + H^+].

5-(2-Pyrrolyl)-5,10,15-tris[(4-trifluoromethyl)phenyl]isocorrole: Yield 6.1 mg (30 %). UV-Vis (CH_2Cl_2) λ_{max} (nm) [ϵ x 10^{-4} ($M^{-1}cm^{-1}$)]: 338 (2.71), 407 (4.06), 661 (0.73), 706 (0.74). ^{1}H NMR (400 MHz, $CDCl_3$, δ): 14.75 (s, 2H, NH), 8.11 (s, 1H, 1-pyrrolyl), 7.77 – 7.69 (m, 4H, overlapping 10-*m*-Ph and 15-*m*-Ph), 7.67 (d, J = 8.0 Hz, 2H, 15-*o*-Ph), 7.61 (d, J = 7.9 Hz, 2H, 10-*o*-Ph), 7.53 (d, J = 8.2 Hz, 2H, 5-*m*-Ph), 7.36 (d, J = 8.2 Hz, 2H, 5-*o*-Ph), 7.01 (d, 2H, 2 overlapping β-H), 6.70 – 6.67 (m, 2H, overlapping 5-pyrrolyl and β-H), 6.58 (d, J = 4.6 Hz, 1H, β-H), 6.40 – 6.36 (m, 2H, 2 overlapping β-H), 6.20 (dd, J = 4.3, 2.4 Hz, 1H, β-H), 6.18 – 6.15 (m, 1H, 4-pyrrolyl), 6.15 – 6.11 (m, 1H, 3-pyrrolyl), 5.95 (dd, J = 3.6, 2.5 Hz, 1H, β-H). MS (ESI) m/z: 796.2114; calcd for $C_{44}H_{26}N_5F_9H$: 796.2117 [M + H^+]. Elemental analysis (%): C 66.62, H 3.42, N 8.69; calcd for $C_{44}H_{26}N_5F_9$: C 66.42, H 3.29, N 8.80.

10-(2-Pyrrolyl)-5,10,15-tris[(4-trifluoromehtyl)phenyl]isocorrole: Yield 0.4 mg (2.0 %). UV-Vis (CH_2Cl_2) λ_{max} (nm) [ϵ x 10^{-4} ($M^{-1}cm^{-1}$)]: 347 (0.89), 429 (1.94), 648 (0.29), 700 (0.26). ^{1}H NMR (400 MHz, $CDCl_3$ δ): 14.58 (s, 2H, NH), 7.86 (s, 1H, 1-pyrrolyl), 7.71 – 7.62 (m, 8H, overlapping 5,15-*o*-Ph and 5,15-*m*-Ph), 7.50 (d, J = 8.2 Hz, 2H, 10-*m*-Ph), 7.15 (d, J = 8.2 Hz, 2H, 10-*o*-Ph), 6.72 (d, J = 4.2 Hz, 2H, β-H), 6.67 – 6.61 (m, 3H, overlapping β-H and 2-pyrrolyl), 6.50 (d, J = 4.3 Hz, 2H, β-H), 6.06 (q, J = 3.0 Hz, 1H, 3-pyrrolyl), 5.90 (d, J = 4.3 Hz, 2H, β-H), 5.79 (d, J = 3.9 Hz, 1H, 4-pyrrolyl). MS (ESI) m/z: 796.2112; calcd for $C_{44}H_{26}N_5F_9H$: 796.2117 [M + H^+].

General procedure for preparation of copper 5/10-(2-pyrrolyl)triarylisocorroles. To a 100 ml round-bottom flask equipped with a magnetic stirring bar was added free-base isocorrole (15-25 mg, mixture of isomers), $Cu(OAc)_2 \cdot H_2O$ (1.5 eq), $CHCl_3$ (8 mL) and MeOH (2 mL). The mixture was refluxed for 30 minutes (room temperature for *p*-CF_3). The solvents were removed under vacuum and the solids passed through silica with dichloromethane. Separation of 5- and 10-isomers required preparative thin-layer chromatography employing DCM for *p*-OCH_3, DCM/pentane (1:1) for *p*-CH_3, and DCM/pentane (1:2) for *p*-H and *p*-CF_3. In the event the isomers did not separate, the copper isocorrole band was divided in fractions and prep-TLC repeated on each individual fraction. The process continued until full separation was

achieved. Yields and analytical details for each compound are as follows. Due to low yield of the 10-isomers, elemental analysis was only done for the 5-isomers.

Copper 5-(2-pyrrolyl)-5,10,15-tris(4-methoxyphenyl)isocorrole: Yield 9.2 mg (54 %). UV-Vis (CH_2Cl_2) λ_{max} (nm) [ϵ x 10^{-4} ($M^{-1}cm^{-1}$)]: 368 (2.42), 459 (3.80), 556 (0.69), 786 (0.59), 862 (0.77). MS (ESI) m/z: 742.1869; calcd for $C_{44}H_{33}N_5O_3Cu$: 742.1874 [M^+]. Elemental analysis (%): C 71.19, H 4.70, N 9.03; calcd for $C_{44}H_{33}N_5O_3Cu$: C 71.10, H 4.47, N 9.42.

Copper 10-(2-pyrrolyl)-5,10,15-tris(4-methoxyphenyl)isocorrole: Yield 0.9 mg (5.3 %). UV-Vis (CH_2Cl_2) λ_{max} (nm) [ϵ x 10^{-4} ($M^{-1}cm^{-1}$)]: 271 (1.38), 387 (2.76), 470 (3.50), 544 (0.34), 726 (0.34), 800 (0.78). MS (ESI) m/z: 742.1876; calcd for $C_{44}H_{33}N_5O_3Cu$: 742.1874 [M^+].

Copper 5-(2-pyrrolyl)-5,10,15-tris(4-methylphenyl)isocorrole: Yield 21.7 mg (77 %). UV-Vis (CH_2Cl_2) λ_{max} (nm) [ϵ x 10^{-4} ($M^{-1}cm^{-1}$)]: 285 (1.60), 361 (3.00), 459 (3.61), 557 (0.65), 793 (0.65), 860 (0.85). MS (ESI) m/z: 694.2032; calcd for $C_{44}H_{33}N_5Cu$: 694.2026 [M^+]. Elemental analysis (%): C 75.41, H 5.06, N 9.61; calcd for $C_{44}H_{33}N_5Cu$: C 76.00, H 4.78, N 10.07.

Copper 10-(2-pyrrolyl)-5,10,15-tris(4-methylphenyl)isocorrole: Yield 1.5 mg (5.3 %). UV-Vis (CH_2Cl_2) λ_{max} (nm) [ϵ x 10^{-4} ($M^{-1}cm^{-1}$)]: 315 (1.23) 370 (2.81), 468 (3.49), 539 (0.38), 728 (0.33), 800 (0.80). MS (ESI) m/z: 694.2031; calcd for $C_{44}H_{33}N_5Cu$: 694.2026 [M^+].

Copper 5-(2-pyrrolyl)-5,10,15-triphenylisocorrole: Yield 14.7 mg (73 %). UV-Vis (CH_2Cl_2) λ_{max} (nm) [ϵ x 10^{-4} ($M^{-1}cm^{-1}$)]: 296 (1.41), 357 (2.68), 459 (3.13), 557 (0.57), 792 (0.58), 856 (0.80). MS (ESI) m/z: 652.1558; calcd for $C_{41}H_{27}N_5Cu$: 652.1557 [M^+]. Elemental analysis (%): C 75.44, H 4.57, N 10.25; calcd for $C_{41}H_{27}N_5Cu$: C 75.38, H 4.17, N 10.72.

Copper 10-(2-pyrrolyl)-5,10,15-triphenylisocorrole: Yield 1 mg (5.0 %). UV-Vis (CH_2Cl_2) λ_{max} (nm) [ϵ x 10^{-4} ($M^{-1}cm^{-1}$)]: 305 (0.87), 361 (1.28), 470 (1.96), 540 (0.21), 729 (0.18), 800 (0.44); MS (ESI) m/z: 652.1556; calcd for $C_{41}H_{27}N_5Cu$: 652.1557 [M^+].

Copper 5-(2-pyrrolyl)-5,10,15-tris[(4-trifluoromethyl)phenyl]isocorrole: Yield 11.6 mg (48 %). UV-Vis (CH_2Cl_2) λ_{max} (nm) [ϵ x 10^{-4} ($M^{-1}cm^{-1}$)]: 308 (1.83), 357 (2.67), 465 (3.44), 560 (0.63), 792 (0.67), 858 (0.98). MS (ESI) m/z: 856.1171; calcd for $C_{44}H_{24}N_5F_9Cu$: 856.1179 [M^+]. Elemental analysis (%): C 61.17, H 3.06, N 7.70; calcd for $C_{44}H_{24}N_5F_9Cu$: C 61.65, H 2.82, N 8.17.

Copper 10-(2-pyrrolyl)-5,10,15-tris[(4-trifluoromethyl)phenyl]isocorrole: Yield 1.2 mg (5.0 %). UV-Vis (CH_2Cl_2) λ_{max} (nm) [ϵ x 10^{-4} ($M^{-1}cm^{-1}$)]: 302 (1.42), 356 (1.39), 388 (1.31), 474 (2.62), 545 (0.24), 734 (0.27), 806 (0.62). MS (ESI) m/z: 856.1173; calcd for $C_{44}H_{24}N_5F_9Cu$: 856.1179 [M^+].

Single-crystal X-ray structure determination. **X-ray structure determination**. Suitable crystals were obtained by diffusion of methanol vapor into concentrated solutions of H_2[5-pyr-T*p*OMePiC] in dichloromethane and Cu[10-pyr-T*p*OMePiC] in chloroform. X-ray data were collected on beamline 12.2.1 at the Advanced Light Source of Lawrence Berkeley National Laboratory, Berkeley, California. The samples were mounted on MiTeGen® kapton loops and placed in a 100(2) K nitrogen cold stream provided by an Oxford Cryostream 700 Plus low temperature apparatus on the goniometer head of a Bruker D8 diffractometer equipped with PHOTONII CPAD detector. Diffraction data were collected using synchrotron radiation monochromated with silicon(111) to a wavelength of 0.7749(1) Å. In each case, an approximate full-sphere of data was collected using 1° ω scans. Absorption corrections were applied using SADABS.[33] The structure was solved by intrinsic phasing (SHELXT)[34] and refined by full-matrix least squares on F^2 (SHELXL-2014)[35] using the ShelXle GUI.[36] All non-hydrogen atoms were refined anisotropically. Hydrogen atoms were geometrically calculated and refined as riding atoms.

Acknowledgement. This work was supported by the Research Council of Norway (grant no. 262229 to AG) and by the Advanced Light Source, Berkeley, California. The Advanced Light Source is supported by the Director, Office of Science, Office of Basic Energy Sciences, of the U.S. Department of Energy under Contract No. DE-AC02-05CH11231.

References

[1] R. Orlowski, D. Gryko and D. T. Gryko, *Chem. Rev*., 2017, **117**, 3102-3137.

[2] A. Ghosh, *Chem. Rev*., 2017, **117**, 3798-3881.

[3] R. D. Teo, J. Y. Hwang, J. Termini, Z. Gross and H. B. Gray, *Chem. Rev.* 2017, **117**, 2711–2729.

[4] G. Pomarico, X. Xiao, S. Nardis, R. Paolesse, F. R. Fronczek, K. M. Smith, Y. Fang, Z. Ou and K. M. Kadish, *Inorg. Chem*., 2010, **49**, 5766-5774.

[5] R. Costa, G. R. Geir, III and C. J. Ziegler, *Dalton Trans*., 2011, **40**, 4384-4386.

[6] M. Hoffmann, B. Cordes, C. Kleeberg, P. Schweyen, B. Wolfram and M. Bröring, *Eur. J. Inorg Chem*. 2016, 3076–3085.

[7] K. E. Thomas, C. M. Beavers, K. J. Gagnon and A. Ghosh, *ChemistryOpen* 2017, **6**, 402-409.

[8] S. Nardis, G. Pomarico, F. Mandoj, F. R. Fronczek, K. M. Smith and R. Paolesse, *J Porphyrins Phthalocyanines,* 2010, **14**, 752-757.

[9] S. Nardis, G. Pomarico, F. R. Fronczek, M. G. H. Vicente and R. Paolesse, *Tetrahedron Lett.* 2007, **48**, 8643-8646.

[10] D. Sakow, B. Böker, K. Brandhorst, O. Burghaus and M. Bröring, *Angew. Chem., Int. Ed*., 2013, **52**, 4912–4915.

[11] B. Umasekhar, V. S. Shetti and M. Ravikanth, *RSC Adv*., 2018, **8**, 21100–21132.

[12] M. Bröring, S. Köhler and C. Pietzonka, *J. Porphyrins Phthalocyanines*, 2012, **16**, 641–650.

[13] D. Sakow, D. Baabe, B. Böker, O. Burghaus, M. Funk, C. Kleeberg, D. Menzel, C. Pietzonka and M. Bröring, *Chem. –Eur. J*., 2014, **20**, 2913–2924.

[14] S. Winstein, *J. Am. Chem. Soc.* 1959, **81**, 6524–6525.

[15] C. Foroutan-Nejad, S. Larsen, J. Conradie and A. Ghosh, *Sci. Rep*. 2018, **8**, 11952.

[16] C. Foroutan-Nejad and A. Ghosh, *ACS Omega* 2018, **3**, 15865–15869

[17] Several pyrrole-appended porphyrinoid macrocycles are reported in the literature.[18-19]

[18] M. Pawlicki, I. Kańska and L. Latos-Grażyński, *Inorg. Chem*., 2007, **46**, 6575–6584, and references therein.

[19] M. Li, P. Wei, M. Ishida, X. Li, M. Savage, R. Guo, Z. Ou, S. Yang, H. Furuta and Y. Xie, *Angew. Chem. Int. Ed*., 2016, **55**, 3063-3067.

[20] A. Ghosh, *Angew. Chem. Int. Ed*. 2004, **43**, 1918-1931.

[21] I. H. Wasbotten, T. Wondimagegn and A. Ghosh, *J. Am. Chem. Soc.* 2002**, 124**, 8104-8116.

[22] M. Bröring, F. Bregier, E. C. Tejero, C. Hell and M. C. Holthausen, *Angew. Chem., Int. Ed.* 2007, **46**, 445–448.

[23] A. B. Alemayehu, E. Gonzalez, L. K. Hansen and A. Ghosh, *Inorg. Chem.* 2009, **48**, 7794–7799.

[24] K. E. Thomas, J. Conradie, L.-K. Hansen and A. Ghosh, *Eur. J. Inorg. Chem.* 2011, 1865–1870.

[25] A. B. Alemayehu, L.-K. Hansen and A. Ghosh, A. Nonplanar, Noninnocent, and Chiral: A Strongly Saddled Metallocorrole. *Inorg. Chem.* 2010, **49**, 7608-7610.

[26] K. E. Thomas, H. Vazquez-Lima, Y. Fang, Y. Song, K. J. Gagnon, C. M. Beavers, K. M. Kadish and A. Ghosh, *Chem. Eur. J.* 2015, **21**, 16839-16847.

[27] K. E. Thomas, L. J. McCormick, D. Carrié, H. Vazquez-Lima, G. Simonneaux and A. Ghosh, *Inorg. Chem*., 2018, **57**, 4270–4276.

[28] S. Berg, K. E. Thomas, C. M. Beavers and A. Ghosh, *Inorg. Chem.* **2012,** *51*, 9911-9916.

[29] I. K. Thomassen, L. J. McCormick and A. Ghosh, *ACS Omega*, 2018, **3**, 5106-5110.

[30] K. E. Thomas, A. B. Alemayehu, J. Conradie, C. M. Beavers and A. Ghosh, *Acc. Chem. Res.* 2012, **45**, 1203-1214.

[31] B. Koszarna and D. T. Gryko, *J. Org. Chem*. 2006, **71**, 3707-3717.

[32] Many metalloporphyrins and metallocorroles, in particular hemes and Mn and Fe corroles do not yield satisfactory elemental analyses. Others, such as coinage metal corroles, do so readily. The present complexes turned out to be intermediate. Although the majority of analyses proved to be within 0.5% of their theoretical values, a few exhibited errors of 1-2%. Although the latter can be accounted for by assuming tightly held solvent molecules, the theoretical analyses quoted here refer to simply the solvent-free molecular formulas.

[33] Krause, L.; Herbst-Irmer, R.; Sheldrick, G. M.; Stalke, D. Comparison of silver and molybdenum microfocus X-ray sources for single-crystal structure determination. *J. Appl. Cryst*. **2015**, *48*, 3-10.

[34] Sheldrick, G. M. SHELXT - Integrated Space-Group and Crystal-Structure Determination. *Acta Cryst*. **2015**, *A71*, 3-8.

[35] Sheldrick, G. M. Crystal Structure Refinement with SHELXL. *Acta Cryst*. **2015**, *C71*, 3-8.

[36] Hübschle, C. B.; Sheldrick, G. M.; Dittrich, B. ShelXle: a Qt graphical user interface for SHELXL. *J. Appl. Cryst*. **2011**, *44*, 1281-1284.